Microchemical Journal 218 (2025) 115468

Contents lists available at ScienceDirect

Microchemical Journal

journal homepage: www.elsevier.com/locate/microc

Untargeted fluorescence spectroscopy for the quantification of added caramel (E-150d) in presence of natural caramel in Aceto Balsamico di Modena PGI

Samuele Pellacani [a], Monica Casale [b], Beatriz Quintanilla Casas [c], Rasmus Bro [c], Franca Ladogana [d], Federico Desimoni [d], Marina Cocchi [a], Caterina Durante [a,*], Daniele Tanzilli [a], Lorenzo Strani [a]

[a] Department of Chemical and Geological Sciences, University of Modena and Reggio Emilia, via Campi 103, 41125 Modena, Italy
[b] Department of Pharmacy, University of Genoa, Viale Cembrano, 4 – University of Genoa, via Dodecaneso 31, Genoa 16148, Italy
[c] Department of Food Science, University of Copenhagen, Rolighedsvej 30, Frederiksberg C DK-1958, Denmark
[d] Consorzio Tutela Aceto Balsamico di Modena, Via Ganaceto 113, Modena 41121, Italy

ARTICLE INFO

Keywords:
Aceto Balsamico di Modena PGI
Synthetic caramel
Excitation-emission fluorescence spectroscopy
Parallel factor analysis
Partial least square regression
Food authentication

ABSTRACT

Synthetic caramel (E-150d) is a permitted colorant in Aceto Balsamico di Modena with Protected Geographical Indication (ABM PGI), used for colour stabilization and requiring label declaration. However, caramel-like compounds also occur naturally due to the cooked must use in balsamic vinegar production, when cooked grape must is used as one of the raw materials. Currently, no official method distinguishes between added and natural caramel in ABM PGI. To address this, we investigated excitation-emission fluorescence spectroscopy as a rapid analytical tool. Three-way Excitation-Emission Matrices (EEMs) were acquired for various ABM samples and their raw materials, including those spiked with synthetic caramel and commercial products. Parallel Factor Analysis (PARAFAC) was applied to the EEM data to identify and resolve fluorescent components associated with both natural and synthetic caramel. The scores from the PARAFAC model were then used to build a Partial Least Squares Regression (PLS) model for quantifying the added caramel concentration. The developed method showed good accuracy in quantifying the synthetic caramel content in spiked samples and a blind test of commercial ABM, with satisfactory reproducibility over time. This study provides a promising untargeted fluorescence-based approach for the detection and quantification of synthetic caramel in ABM PGI, offering a valuable tool for quality control and authenticity verification.

1. Introduction

Aceto Balsamico di Modena (ABM), is a traditional product deeply rooted in the culture and history of Modena and obtained Protected Geographical Indication (PGI) status in 2009 [1]. This designation ensures the exceptional quality of this vinegar, recognized for its unique and unmistakable flavour. Beyond its culinary value, ABM holds significant social and economic importance in Italy, providing income for numerous producers and representing a cornerstone of the country's gastronomic tradition.

ABM PGI is produced using simple yet carefully selected ingredients in accordance with strict PGI regulations. The raw materials used for its production are concentrated grape must and/or concentrated cooked grape must (at least 20 %), aged vinegar (at least 10 years old), and wine vinegar (at least 10 %). Acetification and aging occur in fine wooden casks—oak, chestnut, mulberry, or juniper—for a minimum of 60 days. Products aged for at least three years are classified as "aged." During production, caramel compounds can naturally form through Maillard reactions and caramelization during the cooking of grape must [2,3]. However, regulations also permit the addition of caramel (up to 2 % by weight) as a colouring stabilizer. The use of caramel must not alter the vinegar's sensory properties and must be clearly declared on the label; otherwise, its undeclared presence constitutes fraud.

Caramel can be obtained by controlled heat treatment of food carbohydrates, often with the addition of acids or alkalis. Several types of caramel are authorized for food use. From a food market legislation

* Corresponding author.
E-mail address: caterina.durante@unimore.it (C. Durante).

https://doi.org/10.1016/j.microc.2025.115468
Received 11 July 2025; Received in revised form 19 September 2025; Accepted 20 September 2025
Available online 23 September 2025

perspective, it is considered a colouring agent that must be listed on the food label with a specific code: the letter E-150 followed by a letter (a-d) depending on the caramel's synthesis method. Among the various colour additives available, sulphite-ammonia caramel (E-150d) is the most widely used in the production of ABM PGI. It is produced by heating sugar solutions, such as concentrated grape must, in the presence of sulphites (e.g., sodium sulphite) and ammonia-containing compounds, promoting caramelization and affecting the final colour. However, the chemical composition of caramel is strictly dependent on its production process. Caramelization is a complex process characterized by several steps that can lead to the formation of different products. During caramelization, carbohydrates are decomposed, dehydrated, and polymerized at high temperatures, and the resulting products are closely related to the temperature and type of starting carbohydrate. For example, caramelization begins at approximately 105 °C for fructose, 150 °C for glucose, 170 °C for sucrose, and 180 °C for maltose [4]. The characterization of the final product after caramelization is somewhat complex, as it can be a mixture of different dehydrated polymers depending on the initial sugars [4,5].

The detection of E-150d in ABM, particularly distinguishing it from naturally formed caramel, has been the focus of the present study. Several targeted [6–9] and untargeted [10–12] techniques have been employed for the identification of caramel in food products, highlighting the complexity of obtaining reliable results. In targeted studies, the presence of caramel is correlated with the presence of several markers, including many belonging to the furfural family [13]. However, these markers are not adequate to distinguish synthetic from natural caramel in ABM, as they may also be present in the latter if cooked grape must is used as a raw material [14]. In 2012, Golon & Kuhnert [7] utilized advanced high-resolution mass spectrometry and liquid chromatography-tandem mass spectrometry to characterize caramel composition. They identified thousands of compounds formed by heating glucose, fructose, and sucrose, including carbohydrate oligomers, dehydration and hydration products, disproportionation products, and aromatic compounds such as diacetyl, furfurals (e.g., hydroxymethylfurfural), furanones, and maltol.

The same critical issues extend to untargeted studies. Indeed, Reina et al. developed two analytical methods—one based on excitation and emission fluorescence [10] and another on UV–Vis spectroscopy [12], combined with chemometric data analysis—to identify and quantify E-150d in Balsamic Vinegar of Modena and Spanish PDO vinegars. In 2022, Shamsi et al. proposed laser-induced fluorescence spectroscopy as a rapid technique to determine and quantify the amount of grape-must caramel used in the production of balsamic vinegar [11]. Notwithstanding the satisfactory results obtained in all these studies, they did not focus on evaluating the potential of these methods to distinguish balsamic vinegar with added E-150d from that with naturally occurring caramel. As such, our work represents the first attempt specifically aimed at addressing this current and significant issue, both for the Consortium of Balsamic Vinegar of Modena and for consumers.

This study aimed to develop an accurate and rapid method based on fluorescence spectroscopy for the identification of samples with added caramel, to provide essential support to regulatory bodies verifying this product's authenticity. Fluorescence spectroscopy offers several advantages over other spectroscopic techniques, including superior selectivity, high sensitivity to a broad range of analytes, and minimal or even no sample preparation [15]. It has been widely utilized in food analysis as a competitive, highly sensitive, rapid, and non-destructive analytical method [16–18]. However, a carefully designed experimental strategy needs to be applied to address the challenges posed by the complex matrix of balsamic vinegar, including high viscosity, density, and optical interference. ABM PGI samples free of E-150d were spiked with varying amounts of the additive. Commercial ABM PGI samples, which may contain undeclared caramel, were also analysed to test the model's accuracy. Three-way Excitation-Emission Matrix (EEM) data were preprocessed using Parallel Factor Analysis (PARAFAC) [19], a multiway method that resolves fluorescence data into independent components representing potential fluorophores and their relative concentrations. Finally, a first attempt to quantify the amount of E-150d in the vinegar samples was made using Partial Least Squares Regression (PLS) [20] applied to the PARAFAC scores.

An important key aspect of this study is the rigorous development of the analytical protocol, which encompasses both the sampling process (i.e., the selection of samples to be analysed) and the planning of the spectroscopic measurements. Regarding sampling, vinegars exhibiting a broad range of densities and aging processes were selected, despite challenges in sample availability, to ensure a representative and comprehensive analytical dataset. The selection comprised both recently produced and long-aged samples, characterized by differing density and concentrations. This approach was designed to account for the main potential sources of variability among vinegar producers that may influence the chemical composition of the vinegar samples and thus the reliability of the results.

Additionally, selected aged samples were analysed during two separate analytical sessions (one in spring/summer and the other in autumn/winter) to evaluate the robustness and temporal stability of the models. Indeed, spectroscopic methods are known to be influenced by environmental conditions, particularly temperature and humidity.

2. Experimental section

2.1. Sampling

The analysed specimens included various types of vinegar and raw materials from five different producers: 10-year aged vinegar (1 producer), 3-year aged vinegar (4 producers representing a range of densities and raw materials), 1.5-year aged intermediate vinegar (2 producers), 60-days aged vinegar (4 producers), cooked must (3 producers), and wine vinegar (2 producers). This resulted in a total of 16 initial specimens. To assess the impact of synthetic caramel (E-150d), these specimens were spiked with different concentrations (0 %, 0.5 %, 1 %, 1.5 %, 2 %, and 3 %). The 0 % spiked specimens were analysed in duplicate, resulting in 112 samples (7 spikes × 16 specimens). Additionally, the 3-year aged vinegars (3 specimens, A, B and C) and their spiked counterparts (7 spikes, 0–3 %) were analysed twice, once upon collection and again after six months, to evaluate the method's reproducibility over time (see section 3.2). Furthermore, a blind set of six commercial vinegars, declared containing synthetic caramel at concentrations below 2 %, was analysed once upon collection and again after six months. The full list of analysed samples is provided in Table 1.

2.2. Samples preparation and spectroscopic analysis

Prior to the spectroscopic measurements, all samples were diluted with deionized water to get an absorbance <2.0, as suggested to minimize the inner filtering effects (IFE) and make the absorbance correction accurate [19–21]. The samples were diluted 1000 times [22].

Fluorescence measurements were conducted at room temperature on a Perkin-Elmer LS55B luminescence spectrometer (Waltham, MA, USA) equipped with a 150-W xenon arc lamp with a right-angle geometry. A 1 cm quartz cuvette (101-QS SUPRASIL® High-Precision Cells, Hellma GmbH & Co. KG, Müllheim, Germany), with 10 mm path length and 3.50 mL inner volume was used for the analysis. Emission scans were performed from 300 to 700 nm at 1 nm steps, with excitation wavelengths from 250 to 650 nm at 10 nm increments. Emission and excitation slits were set at 5 nm and the scanning speed was maintained at 1200 nm/min for all the acquisitions.

In order to correct the fluorescence spectra for the inner filter effects (see section 2.3.1), the UV–Visible absorbance spectra on each sample were also acquired, using a UV–Vis spectrometer (Cary-100 double-ray UV–Vis spectrometer, Agilent) from $\lambda = 200$ to 800 nm and using Millipore water as blank with 1 cm quartz cuvette.

Table 1
Investigated specimens, raw materials and their respective density values.

	Producer	Specimen type	Raw materials	Density (g/cm^3)
Specimens used for building and validating the model	**A**	60-days aged vinegar	Cooked must and wine vinegar	1.07
		3-year aged vinegar	Cooked must and wine vinegar	1.25
		10-year aged vinegar	Cooked must and wine vinegar	1.30
		Cooked must	/	/
		Wine vinegar	/	/
	B	3-year aged vinegar	Cooked must and wine vinegar	1.33
		Cooked must	/	/
	C	60-days aged vinegar	Cooked must and wine vinegar	1.18
		1.5-year aged vinegar	Cooked must and wine vinegar	1.18
		3-year aged vinegar	Cooked must and wine vinegar	1.18
		Cooked must	/	/
		Wine vinegar	/	/
	D	60-days aged vinegar	Concentrated must and wine vinegars	1.07
	E	60-days aged vinegar	Cooked must and wine vinegar	1.35
		1.5-year aged vinegar	Cooked must and wine vinegar	1.35
		3-year aged vinegar	Cooked must and wine vinegar	1.35
Blind test	**F**	3-year aged vinegar	Cooked must, wine vinegar and E-150d	1.065
	G	3-year aged vinegar	Cooked must, wine vinegar and E-150d	1.115
	H	3-year aged vinegar	Cooked must, wine vinegar and E-150d	1.10
	I	3-year aged vinegar	Cooked must, wine vinegar and E-150d	1.08
	L	3-year aged vinegar	Cooked must, wine vinegar and E-150d	N.A.
	M	3-year aged vinegar	Cooked must, wine vinegar and E-150d	N.A.

2.3. Data analysis

2.3.1. Preprocessing

The EEM data were organized in a three-way array (sample × emission wavelengths × excitation wavelengths) and analysed with PARAFAC. However, fluorescence intensity is linearly related to concentration only in very dilute samples (A < 0.05 a.u.) [20]. In other cases, inner-filter effects (IFE) must be corrected. IFE occurs when the sample matrix absorbs radiation, reducing excitation and emitted light. Non-fluorescent chromophores contribute to inner filter effect. As absorbance increases, the non-linearity worsens, potentially leading to decreased fluorescence at higher concentrations. Aceto Balsamico di Modena is very dense and dark, so the inner-filter effect must be eliminated. In this work, two actions were taken in this regard: the samples were diluted 1:1000 (see section 2.2) and the fluorescence data were corrected for the IFE with the function *flucut* (Eigenvector Research Inc., Wenatchee, WA) using the absorbance UV–vis spectra. Moreover, the signals were affected by Rayleigh and Raman scattering [23,24] which are diagonal signals that do not follow the PARAFAC model. The Raman scattering was corrected by subtracting the water signal acquired in every session. Instead, the first- and second- order Rayleigh scattering was corrected using the *flucut* function by replacing the scattering areas with interpolated values. The details of the method are reported elsewhere [25,26]. The method implemented in the *flucut* function requires only the half-width values for the scatters. In this study, 20 and 40 nm were found to be optimal values for removing first- and second-order Rayleigh scattering.

2.3.2. PARAFAC

EEM data are organized in a three-way array (sample × emission wavelengths × excitation wavelengths); the most predominant decomposition methodologies within the class of linear models for unsupervised three-way data have been factor analysis methods such as PARAFAC [27].

The PARAFAC decomposition is expressed as follows:

$$x_{ijk} = \sum_{f=1}^{F} a_{if} b_{jf} c_{kf} + e_{ijk} i = 1, 2, \ldots, \mathrm{I}; j = 1, 2, \ldots, \mathrm{J}; k = 1, 2, \ldots, \mathrm{K} \quad (1)$$

where x_{ijk} are the elements of $\underline{\mathbf{X}}$ tensor for sample i in the corresponding emission j and excitation k wavelength [21]. a_{if} are the elements of the sample mode score matrix **A** ($I \times F$), b_{jf} are the elements of the excitation mode loadings matrix **B** ($J \times F$) and c_{kf} are the elements of the emission mode loadings matrix **C** ($K \times F$). The element e_{ijk} is the residual array in the position i, j, and k of residual tensor (a tensor with the same dimensions as $\underline{\mathbf{X}}$ tensor). The scalar F is the number of PARAFAC components (factors).

In the case of well-working PARAFAC model of fluorescence data, $\mathbf{a}_f$, $\mathbf{b}_f$ and $\mathbf{c}_f$ are the estimates of the f-th fluorophore (component) sample profiles, excitation spectrum and emission spectrum. Sample profile refers to the relative quantity of f-th fluorophore in each sample [28]. Several PARAFAC models were tested with different numbers of factors (from 3 to 6). Finally, the models have been validated considering the core consistency (CORCONDIA, [19]) and the split-half analysis similarity.

2.3.3. PLS from the PARAFAC scores

In the present study, the scores obtained from the PARAFAC model were used to calibrate a partial least squares regression (PLS) model to quantify the synthetic caramel.

Firstly, an exploratory analysis was carried out using PARAFAC (Section 2.3.2). The Kennard–Stone algorithm [29] was then applied to the PARAFAC scores obtained during this exploratory stage, in order to divide the samples into training and test sets. Specifically, the excitation–emission matrix (EEM) dataset (133 samples × 401 emission wavelengths × 41 excitation wavelengths) was split with two-thirds of the samples assigned to the training set (81 samples). Finally, a new PARAFAC model was built using only the training data, and this model was subsequently used to predict the scores of the test and blind samples.

PLS models were cross-validated leaving one product out and the optimal number of latent variables (LVs) was selected based on the lowest root mean square error of cross-validation (RMSECV). A PLS model with 2 LVs was then developed. Mean centering was applied as a preprocessing step. The sum of squared residuals (Q) and Hotelling's T^2 statistics were evaluated for all samples, and no outliers were identified.

2.3.4. Software

The FL WinLab software (PerkinElmer) was used to register the fluorescent signals, and the data were imported to Matlab v. R2024 (The MathWorks, Inc., Natick, MA, US) and PARAFAC and PLSR models were performed using routines in Matlab v. R2024 and PLS_Toolbox v. 9.2 (Eigenvector Research, Inc., Manson, WA, US).

3. Results and discussion

3.1. EEM data

The analysis of EEM data shows interesting differences in the fluorescence excitation/emission spectra depending on the concentration of spiked caramel. These differences are already apparent in the EEM landscapes after a pre-processing step applied for IFE correction and to remove the Rayleigh and Raman scattering (as described in Section 2.3.1).

To demonstrate the efficacy of the IFE removal, we performed PARAFAC analysis on both the raw and corrected data. A five components model was developed and the scores of the third component are reported as example (Fig. S1, Supplementary Materials). In the uncorrected dataset, the samples spiked at 3 % showed highly dispersed scores values (red stars in Fig. S1, Supplementary Materials, ranging from 300 to 4500). After IFE correction, the scores became more consistent, ranging from 2000 to 5000 (blue stars in Fig. S1, Supplementary Materials), thus improving both linearity and comparability across samples. These variations in absolute values can be attributed to the matrix heterogeneity (such as vinegars with varying densities and raw materials, including wine vinegar and cooked must). Consequently, the PLS model was constructed considering the scores of all resolved components, rather than solely the third component. Moreover, examples from different matrices (wine vinegar, balsamic vinegar 60-day and 3-years aged and cooked must) are reported in Fig. S2, Supplementary Materials, showing clear improvement in terms of linearity after the IFE correction.

As an example, Fig. 1 shows the contour plot of the fluorescence landscapes of the 3-year-old aged ABM from Producer C spiked with different concentrations of synthetic caramel. As can be observed, the presence of strongly overlapping fluorescence bands in all EEM landscapes is quite evident and visual inspection indicates that, with the addition of caramel, the fluorescence signal generally increases of intensity, and a new band seems to appear with an excitation around 300 nm and emission around 350–400 nm.

3.2. Evaluation of the intermediate reproducibility

Initially, to assess intermediate reproducibility, the ABM samples (A, B, C) aged for three years were analysed in two independent sessions conducted in different months by different operators. The obtained EEM data were arranged in a three-way data array of dimensions I x J x K, where I is the number of investigated samples (i.e. the 42 samples given by 3 aged vinegar samples x 2 replicates × 7 spikes), J the number of

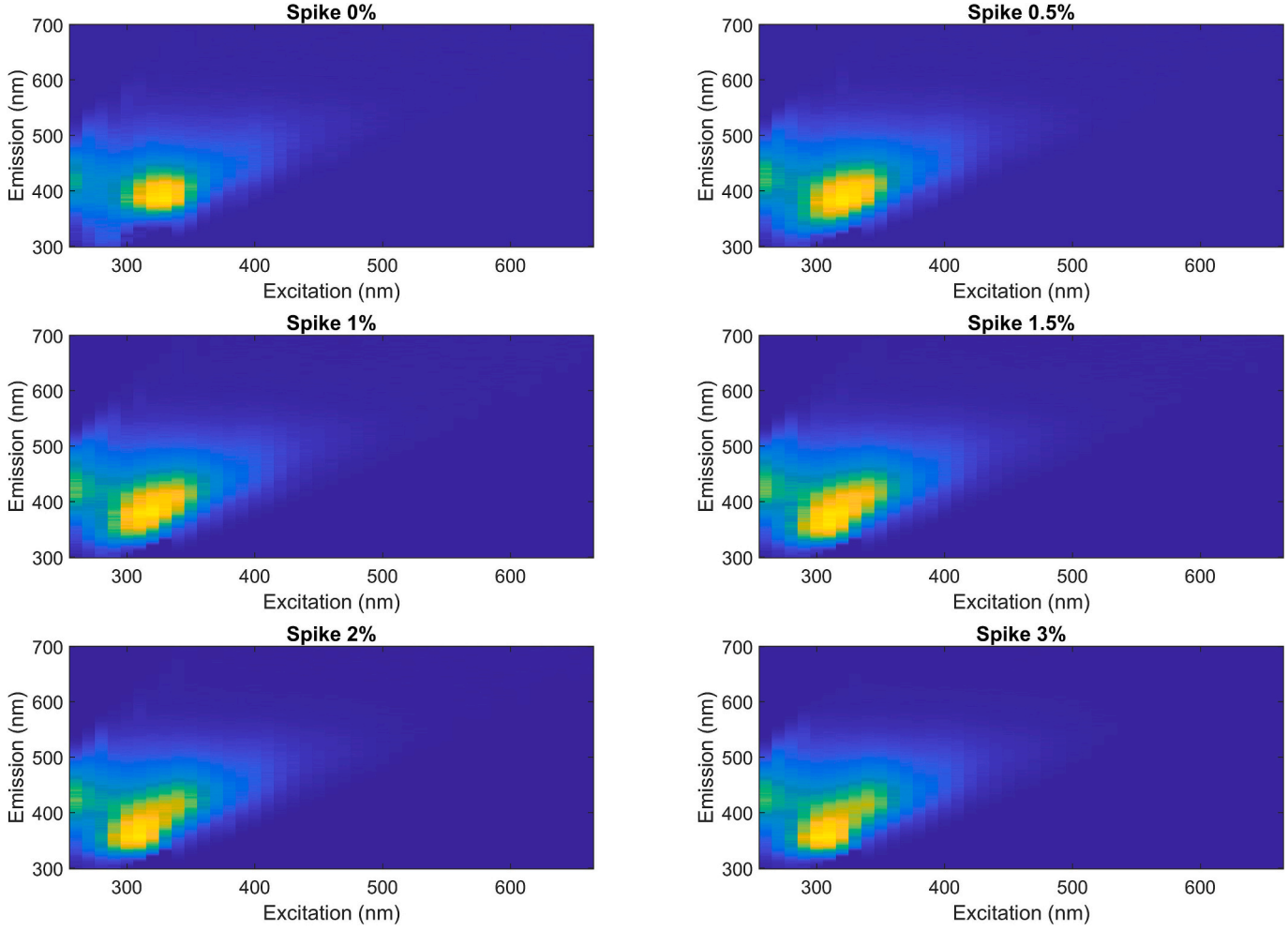

Fig. 1. Fluorescence landscapes of 3-year-old aged balsamic vinegar from Producer C spiked with increasing concentrations of caramel (0 %, 0.5 %, 1 %, 1.5 %, 2 %, 3 %).

emission wavelengths (401 points) and K number of excitation wavelengths (41 points). The development of 3- to 6-component PARAFAC models was then undertaken, and the optimal model in terms of residuals, fit, split-half analysis and core consistency was identified as the one with 5 components.

The scores of the five identified factors are presented in Fig. 2, while the corresponding loadings for emission and excitation modes are provided in the supplementary materials (Fig. S3). As shown in Fig. 2, the results demonstrate good intermediate reproducibility, with the scores of samples analysed in April–March 2024 closely matching those obtained in October 2024. Notably, the sample from Producer C exhibited an increase in the score of the second factor after six months, potentially attributable to continued aging. Additionally, the scores for factors 1, 3, and 5 displayed a consistent upward trend, likely reflecting increased caramel concentration. Based on these encouraging results, the dataset was subsequently expanded to include all specimens listed in Table 1.

3.3. PARAFAC model

Given the good intermediate reproducibility of the analysis, which confirms the stability and reliability of the proposed analytical method, all the fluorescence signals obtained for the samples in Table 1 (excluding the blind test) were analysed together. Therefore, a new three-way array, with 133 samples, 401 emission wavelengths and 41 excitation wavelengths, was built and pre-processed as previously outlined (IFE correction, Rayleigh and Raman scatter removal, and interpolation). The construction of a PARAFAC model was undertaken, and once more, a model comprising five components was determined to be optimal regarding fit, split-half analysis, residuals and core consistency (results reported in Table S1, Supplementary Materials). The loadings of the second (emission spectra) and third (excitation spectra) modes and the sample scores mode are illustrated in Fig. 3. Regarding the scores, the results concerning the third factor (Fig. 3c) are reported in the text, while the others can be seen in Fig. S4, Supplementary Materials, for the sake of brevity. The second and third modes represent the underlying pure spectra of characteristic fluorophores present in the investigated samples. Based on excitation/emission loadings and comparison with previous literature on vinegar and related matrices [10,22], tentative assignments of the detected fluorophores, were made. In particular, Factor 1 (F1, indicated by the blue colour in Fig. 3 a-b) exhibits an excitation maximum between 320 and 340 nm and an emission maximum between 430 and 450 nm. Analogous excitation/emission maxima have been reported from phenolic compounds or products of the Maillard reaction [30,10]. Consequently, these signals may be attributed to compounds present in both vinegar samples, cooked must and caramel. It is important to note that caramel has a highly intricate and largely unexplored composition, which can certainly overlap with that of the investigated samples [10]. In fact, the chemical composition of the synthetic caramel often overlaps significantly with that of "natural caramel", i.e. the caramel produced during the cooking of the must present in the samples. This aspect greatly complicates both the determination and quantification of the synthetic caramel. Factor 2 (F2) shows a peak centred at 300–330 nm in excitation and 360–380 nm in emission (red in Figs. 3 a-b). According to the literature, this factor can be attributed to the presence of phenolic compounds naturally present in wine or to coumarins and tannins released from wood of the barrels during the aging [25]. Factor 4 (F4, violet signal, Fig. 3 a-b) shows maxima at 260–280 nm and 340–360 nm (λ_{ex} and λ_{em}, respectively). This fluorophore may be attributed to the presence of phenolic compounds such as vanillic acid, syringic acid or chlorogenic acid [22]. Factor 5, F5, shows a maximum in excitation at 390–400 nm and a maximum in emission at 490–500 nm (signal in green, Fig. 3 a-b). In literature, this signal was traced back to 5-hydroxymethylfurfural or at least compounds from Maillard reactions [10]. However, it is important to note that, these attributions should be regarded as indicative, since fluorescence is strongly influenced by matrix effects [10] which can shift excitation and emission maxima. Thus, the PARAFAC components are better interpreted as spectral fingerprints of chemical classes rather than unique analytes. Future studies combining fluorescence with complementary analytical techniques (LC-MS) or employing standard addition could provide more definitive confirmation of these assignments.

As regards Factor 3 (F3, yellow signal, Figs. 3 a-b), it appears to be

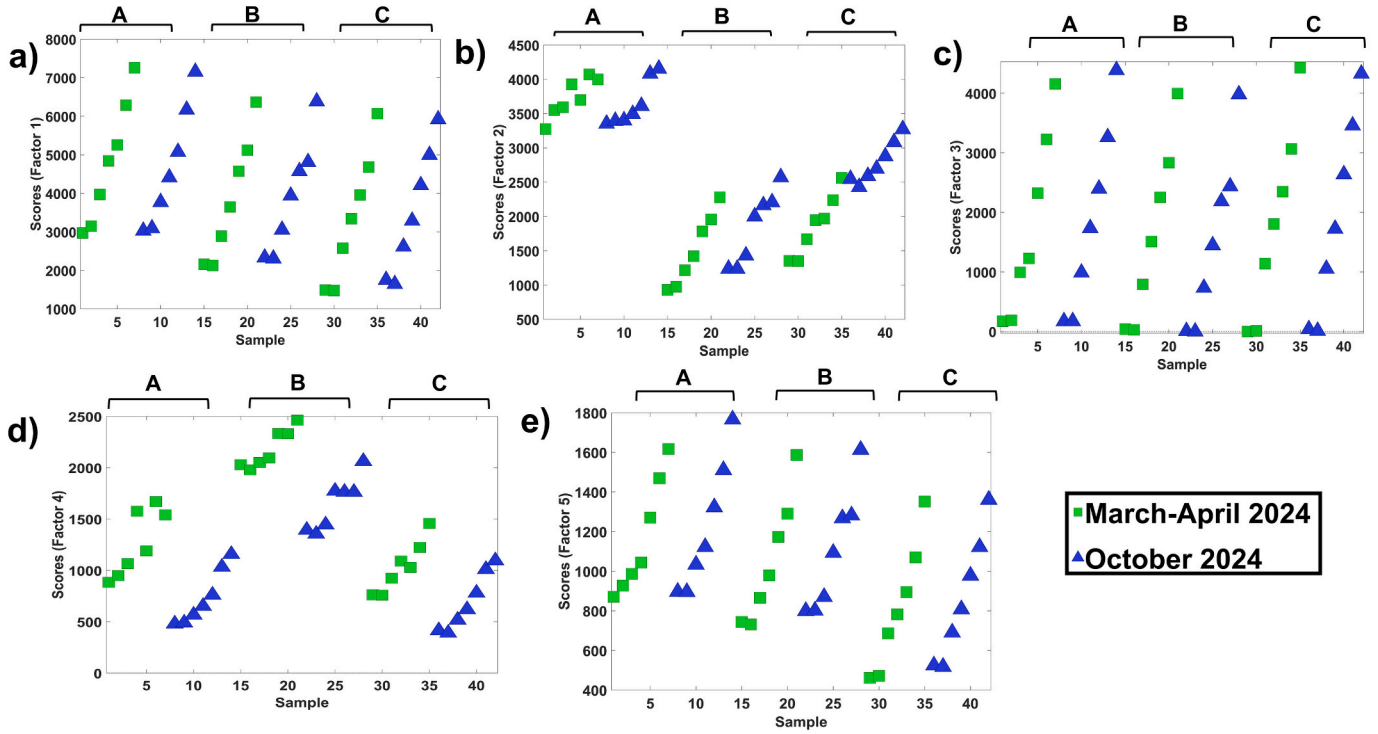

Fig. 2. Scores (a-e) of the five PARAFAC factors versus the samples. The samples are coloured according to the period of analysis.

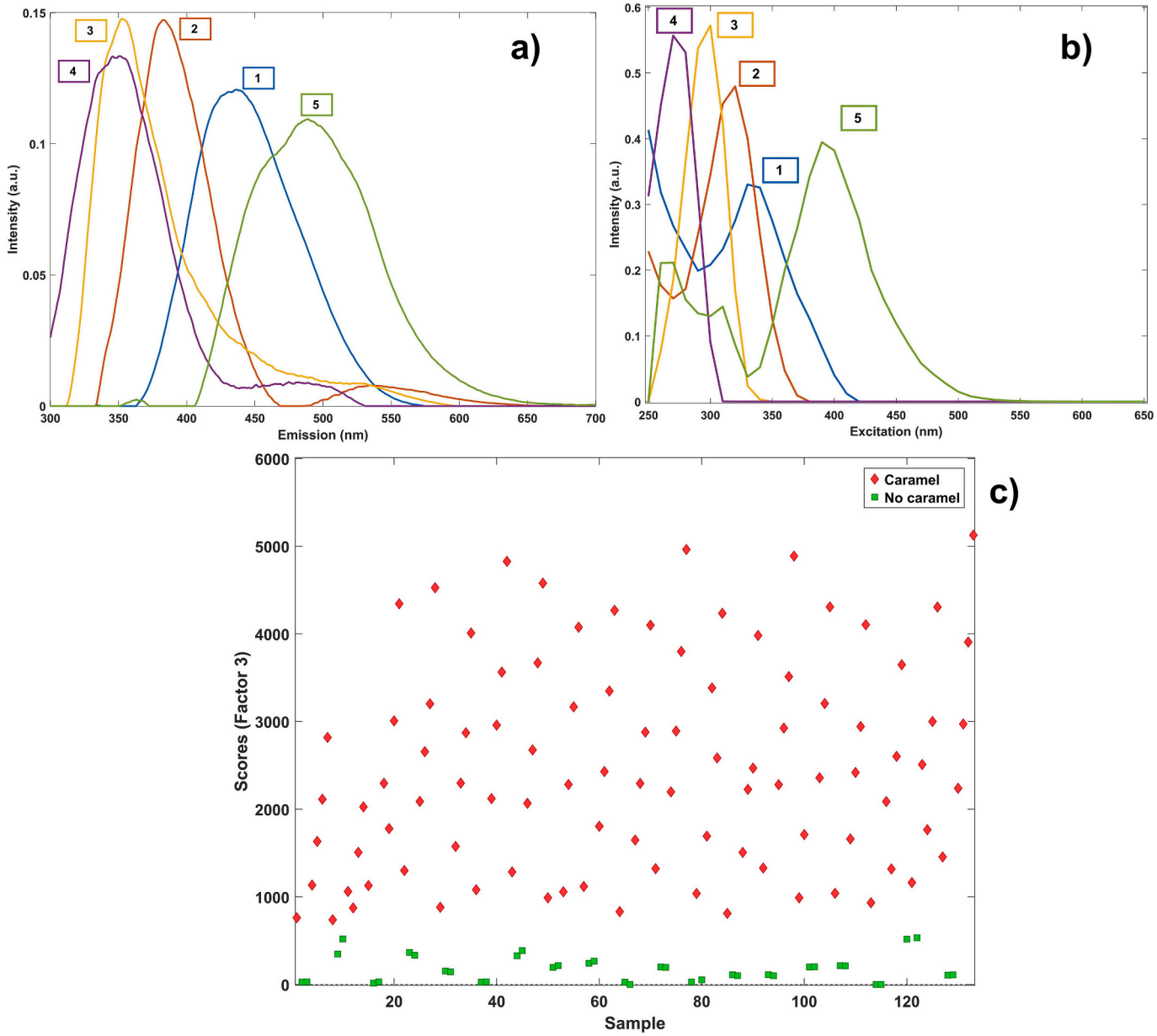

Fig. 3. Loadings of the excitation (a) and emission (b) mode. The scores of factor 3 for all the samples are also reported (c).

associated with a chemical compound characteristic of the presence of synthetic caramel (Fig. 3c). Indeed, the samples of both balsamic vinegar and raw materials (wine vinegar and cooked must), caramel-free (green squares, Fig. 3 c), all demonstrate remarkably low and uniform loadings values. It is evident that as the concentration of added caramel increases, there is a concomitant increase in the score values of all the samples for F3. To further verify the attribution of F3 to synthetic caramel, a pure standard of E-150d was analysed. A 3 % (*w/v*) caramel E-150d solution was prepared, diluted 1:1000, and analysed under the same conditions as the samples. A PARAFAC model with 5 components was developed and the scores of the third factor are reported in Fig. S5, Supplementary Materials. The standard showed high scores, supporting the attribution of this factor to the synthetic caramel. However, it should be noted a strong matrix-effect since the scores of the solutions spiked with 3 % had higher scores than the pure standard (see black circle, Fig. S5). This effect supports the choice to add the standards directly into the vinegar samples rather than performing an external calibration. Overall, this finding underscores the ability of fluorescence spectroscopy to detect caramel. For this reason, a further step involving the prediction of the synthetic caramel by means of PLS was undertaken.

3.4. PLS regression model

Initially, the dataset was divided into calibration and validation sets using the Kennard-Stone algorithm, as explained in Section 2.3.3. This sample selection method ensured a representative subset of 81 samples for model calibration. A PARAFAC model with 5 components were developed. The split-half similarity and core consistency are reported in Table 2 for the training, test and blind set. It could be noted that the core consistency values fall below 50 % in the case of the test and blind set. However, it must be acknowledged that recent studies have shown that core consistency can be an overly conservative diagnostic and may fail when the system is very complex [31]. Therefore, the complexity of the data could be the reason for the relatively low core-consistency value. Subsequently, a PLS model was built using the scores of all five PARAFAC factors as the predictor matrix (X) and the known percentages of added caramel as the response variable (Y). The model reported satisfactory figures of merit, namely coefficients of determination in

Table 2
Results of the PARAFAC and PLS models. The number of factors, the variance explained, and core consistency are reported for the PARAFAC models. The number of latent variables, RMSEC, RMSECV, RMSEP, R^2cal, R^2CV and R^2pred are reported for the PLS models.

PARAFAC (training test)				PARAFAC (test set)		PARAFAC (blind set)		PLS (training set)					PLS (test set)	
Factors	R^2	CC*	SHS^	R^2	CC*	R^2	CC*	LVs	RMSEC	RMSECV	R^2cal	R^2CV	RMSEP	R^2pred
5	99.3	67	77	99.4	30	99.3	32	2	0.29	0.36	0.92	0.91	0.32	0.92

^ Split-half similarity.
* Core consistency.

calibration (R^2cal), cross-validation (R^2CV), and prediction (R^2pred), as well as in the root mean square errors of calibration (RMSEC), cross-validation (RMSECV), and prediction (RMSEP), reported in Table 2.

The model yielded low RMSECV and RMSEP values (0.36 and 0.32, respectively, as shown in Table 2 and graphically showed in Fig. 4) and high correlation coefficients in calibration, cross validation and prediction ($R^2 > 0.91$, Table 2). This approach leveraged the excellent performance of the five PARAFAC factors in differentiating samples based on their synthetic caramel content to build a robust quantitative model. Finally, a blind test was conducted to further validate the developed PLS model. This test involved six commercially available ABM samples, sourced from the market and produced using cooked grape must as a primary raw material, with added caramel at concentrations below the legal limit of 2 %. Importantly, these samples were distinct from the spiked samples used for model calibration and validation, as no artificial spiking was performed on them. To assess the reproducibility of the caramel determination, each of these six blind test samples was analysed in duplicate at six-month intervals. The additive caramel concentrations in these blind samples were predicted using the previously established PLS model. The results of these predictions are detailed in Table S2 (Supplementary Materials). Notably, the predicted caramel concentrations for all six commercial samples were found to be below the 2 % regulatory threshold. The analysis of the duplicate samples over the six-month interval also demonstrated good reproducibility of the method over time.

4. Conclusion

In this study, excitation-emission fluorescence spectroscopy, coupled with PARAFAC and PLS multivariate analysis, has proven to be a rapid, interpretable and effective analytical method for the detection and quantification of synthetic caramel in Aceto Balsamico di Modena PGI. Although this strategy has been employed in the literature, this is the first study in which a systematic analytical strategy has been carried out considering different kinds of samples (balsamic vinegar, cooked must, and wine vinegar), samples in which caramel could be naturally present, as well as the investigation of the analytical procedure over time.

The promising results obtained, including the accurate prediction of caramel concentrations in both spiked samples and a blind test of commercial products, and the demonstrated reproducibility of the method over time, suggest the potential of this methodology for routine quality control and fraud detection within the ABM industry. However, while the set of samples analysed provided a comprehensive dataset for model development, future research should focus on a broader and more diverse set of commercially available ABM products, which would be beneficial to fully validate the robustness and general applicability of the developed model. Furthermore, factors such as variations in production methods across different producers and the fluorescence variability of different cooked grape musts could potentially be studied further. Notwithstanding these considerations, this work contributes to the long-term goal of translating spectroscopic insights into robust analytical tools that can be effectively applied to ensure the quality and authenticity of this valuable Italian food product. The ability to rapidly assess caramel content could be particularly beneficial for regulatory bodies and producers in ensuring compliance with PGI regulations.

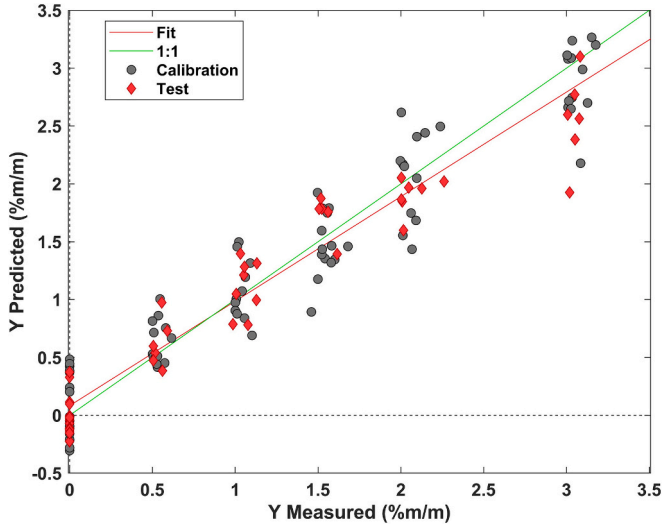

Fig. 4. Plots of predicted versus measured y-values obtained from the PLS model applied to the scores of the 5-factor PARAFAC model.

CRediT authorship contribution statement

Samuele Pellacani: Writing – original draft, Visualization, Validation, Software, Methodology, Investigation, Formal analysis, Data curation, Conceptualization. **Monica Casale:** Writing – original draft, Supervision, Investigation, Conceptualization. **Beatriz Quintanilla Casas:** Writing – original draft, Supervision, Resources. **Rasmus Bro:** Writing – original draft, Supervision, Resources. **Franca Ladogana:** Resources, Funding acquisition. **Federico Desimoni:** Resources, Funding acquisition. **Marina Cocchi:** Supervision, Software, Resources, Funding acquisition. **Caterina Durante:** Writing – original draft, Supervision, Project administration, Investigation, Funding acquisition, Conceptualization. **Daniele Tanzilli:** Software, Resources, Formal analysis. **Lorenzo Strani:** Validation, Software, Resources, Methodology, Investigation.

Declaration of generative AI and AI-assisted technologies in the writing process

During the preparation of this work the authors used ChatGPT-4 in order to improve the overall readability of the paper. After using this tool/service, the authors reviewed and edited the content as needed and take full responsibility for the content of the published article.

Funding sources

The research activity was carried out with a grant from the Ministry of Agriculture (MASAF) under DM No.0291643 dated 6/6/23. S.P. gratefully acknowledges the financial support received through the Erasmus+ Traineeship programme of the European Union, which supported a research stay at the University of Copenhagen.

Declaration of competing interest

The authors declare that they have no known competing financial interests or personal relationships that could have appeared to influence the work reported in this paper.

Appendix A. Supplementary data

Supplementary data to this article can be found online at https://doi.org/10.1016/j.microc.2025.115468.

Data availability

Data will be made available on request.

References

[1] Regulation - 583/2009 - EN - EUR-Lex, (n.d.), https://eur-lex.europa.eu/legal-content/EN/TXT/?uri=CELEX:32009R0583 (accessed July 16, 2024).

[2] M.N. Lund, C.A. Ray, Control of Maillard reactions in foods: strategies and chemical mechanisms, J. Agric. Food Chem. 65 (2017) 4537–4552, https://doi.org/10.1021/acs.jafc.7b00882.

[3] J.M. Ames, Control of the Maillard reaction in food systems, Trends Food Sci. Technol. 1 (1990) 150–154, https://doi.org/10.1016/0924-2244(90)90113-D.

[4] M.P. Luna, J.M. Aguilera, Kinetics of colour development of molten glucose, fructose and sucrose at high temperatures, Food Biophys. 9 (2014) 61–68, https://doi.org/10.1007/s11483-013-9317-0.

[5] T. Kocadağlı, V. Gökmen, Caramelization in foods: A food quality and safety perspective, in: L. Melton, F. Shahidi, P. Varelis (Eds.), Encycl. Food Chem, Academic Press, Oxford, 2019, pp. 18–29, https://doi.org/10.1016/B978-0-08-100596-5.21630-2.

[6] T.R. Kim, S.U. Kim, Y. Shin, J.Y. Kim, S.M. Lee, J.H. Kim, Determination of 4-Methylimidazole and 2-Acetyl-4(5)-tetrahydroxybutylimidazole in caramel color and processed foods by LC-MS/MS, Prev. Nutr. Food Sci. 18 (2013) 263–268, https://doi.org/10.3746/pnf.2013.18.4.263.

[7] A. Golon, N. Kuhnert, Unraveling the chemical composition of caramel, J. Agric. Food Chem. 60 (2012) 3266–3274, https://doi.org/10.1021/jf204807z.

[8] P. Maes, Y.B. Monakhova, T. Kuballa, H. Reusch, D.W. Lachenmeier, Qualitative and quantitative control of carbonated Cola beverages using 1H NMR spectroscopy, J. Agric. Food Chem. 60 (2012) 2778–2784, https://doi.org/10.1021/jf204777m.

[9] M.N. Tzatzarakis, E. Vakonaki, S. Moti, A. Alegakis, C. Tsitsimpikou, I. Tsakiris, M. Goumenou, A.E. Nosyrev, A.K. Rizos, A.M. Tsatsakis, Quantification of 4-Methylimidazole in soft drinks, sauces and vinegars of Greek market using two liquid chromatography techniques, Food Chem. Toxicol. 107 (2017) 565–571, https://doi.org/10.1016/j.fct.2017.03.028.

[10] R. Ríos-Reina, J.A. Ocaña, S.M. Azcarate, J.L. Pérez-Bernal, M. Villar-Navarro, R. M. Callejón, Excitation-emission fluorescence as a tool to assess the presence of grape-must caramel in PDO wine vinegars, Food Chem. 287 (2019) 115–125, https://doi.org/10.1016/j.foodchem.2019.02.008.

[11] E. Shamsi, F. Khalilabadi, Inner filter effect mediated fluorescence properties as a tool to monitor the quantity of grape-must caramel in balsamic vinegar (2022), https://doi.org/10.21203/rs.3.rs-1953256/v1.

[12] R. Ríos-Reina, S.M. Azcarate, J. Camiña, R.M. Callejón, Assessment of UV–visible spectroscopy as a useful tool for determining grape-must caramel in high-quality wine and balsamic vinegars, Food Chem. 323 (2020) 126792, https://doi.org/10.1016/j.foodchem.2020.126792.

[13] A. Piva, C. Di Mattia, L. Neri, G. Dimitri, M. Chiarini, G. Sacchetti, Heat-induced chemical, physical and functional changes during grape must cooking, Food Chem. 106 (2008) 1057–1065, https://doi.org/10.1016/j.foodchem.2007.07.026.

[14] M. Cocchi, G. Ferrari, D. Manzini, A. Marchetti, S. Sighinolfi, Study of the monosaccharides and furfurals evolution during the preparation of cooked grape musts for Aceto Balsamico Tradizionale production, J. Food Eng. 79 (2007) 1438–1444, https://doi.org/10.1016/j.jfoodeng.2006.01.091.

[15] C.M. Andersen, G. Mortensen, Fluorescence spectroscopy: a rapid tool for analyzing dairy products, J. Agric. Food Chem. 56 (2008) 720–729, https://doi.org/10.1021/jf072025o.

[16] R. Karoui, Chapter 7 - spectroscopic technique: Fluorescence and ultraviolet-visible (UV-vis) spectroscopies, in: D.-W. Sun (Ed.), Mod, Academic Press, Tech. Food Authentication Second Ed., 2018, pp. 219–252, https://doi.org/10.1016/B978-0-12-814264-6.00007-4.

[17] A.B. Risum, M. Bevilacqua, C. Li, K. Engholm-Keller, M.M. Poojary, Å. Rinnan, M. N. Lund, Resolving fluorescence spectra of Maillard reaction products formed on bovine serum albumin using parallel factor analysis, Food Res. Int. 178 (2024) 113950, https://doi.org/10.1016/j.foodres.2024.113950.

[18] W. Long, G. Lei, Y. Guan, H. Chen, Z. Hu, Y. She, H. Fu, Classification of Chinese traditional cereal vinegars and antioxidant property predication by fluorescence spectroscopy, Food Chem. 424 (2023) 136406, https://doi.org/10.1016/j.foodchem.2023.136406.

[19] R. Bro, H.A.L. Kiers, A new efficient method for determining the number of components in PARAFAC models, J. Chemometr. 17 (2003) 274–286, https://doi.org/10.1002/cem.801.

[20] S. Wold, H. Martens, H. Wold, The multivariate calibration problem in chemistry solved by the PLS method, in: B. Kågström, A. Ruhe (Eds.), Matrix Pencils, Springer, Berlin, Heidelberg, 1983, pp. 286–293, https://doi.org/10.1007/BFb0062108.

[21] K.R. Murphy, C.A. Stedmon, D. Graeber, R. Bro, Fluorescence spectroscopy and multi-way techniques. PARAFAC, Anal. Methods 5 (2013) 6557–6566, https://doi.org/10.1039/c3ay41160e.

[22] S. Kumar Panigrahi, A. Kumar Mishra, Inner filter effect in fluorescence spectroscopy: as a problem and as a solution, J. Photochem. Photobiol. C Photochem. Rev. 41 (2019) 100318, https://doi.org/10.1016/j.jphotochemrev.2019.100318.

[23] X. Luciani, S. Mounier, R. Redon, A. Bois, A simple correction method of inner filter effects affecting FEEM and its application to the PARAFAC decomposition, Chemom. Intel. Lab. Syst. 96 (2009) 227–238, https://doi.org/10.1016/j.chemolab.2009.02.008.

[24] A.G. Ryder, C.A. Stedmon, N. Harrit, R. Bro, Calibration, standardization, and quantitative analysis of multidimensional fluorescence (MDF) measurements on complex mixtures (IUPAC technical report), Pure Appl. Chem. 89 (2017) 1849–1870, https://doi.org/10.1515/pac-2017-0610.

[25] M. Bahram, R. Bro, C. Stedmon, A. Afkhami, Handling of Rayleigh and Raman scatter for PARAFAC modeling of fluorescence data using interpolation, J. Chemometr. 20 (2006) 99–105, https://doi.org/10.1002/cem.978.

[26] Å. Rinnan, C.M. Andersen, Handling of first-order Rayleigh scatter in PARAFAC modelling of fluorescence excitation–emission data, Chemom. Intel. Lab. Syst. 76 (2005) 91–99, https://doi.org/10.1016/j.chemolab.2004.09.009.

[27] R. Bro, PARAFAC., Tutorial and applications, Chemom. Intel. Lab. Syst. 38 (1997) 149–171, https://doi.org/10.1016/S0169-7439(97)00032-4.

[28] T.-Q. Peng, X.-L. Yin, W. Sun, B. Ding, L.-A. Ma, H.-W. Gu, Developing an excitation-emission matrix fluorescence spectroscopy method coupled with multi-way classification algorithms for the identification of the adulteration of Shanxi aged vinegars, Food Anal. Methods 12 (2019) 2306–2313, https://doi.org/10.1007/s12161-019-01586-5.

[29] R.W. Kennard, L.A. Stone, Computer aided Design of Experiments, Technometrics 11 (1969) 137–148, https://doi.org/10.1080/00401706.1969.10490666.

[30] R. Ríos-Reina, S.M. Azcarate, J.M. Camiña, R.M. Callejón, Sensory and spectroscopic characterization of Argentinean wine and balsamic vinegars: a comparative study with European vinegars, Food Chem. 323 (2020) 126791, https://doi.org/10.1016/j.foodchem.2020.126791.

[31] H.F.F. Halberg, M. Bevilacqua, Å. Rinnan, Is core consistency a too conservative diagnostic? J. Chemometr. 37 (2023) e3483 https://doi.org/10.1002/cem.3483.